



Regular Article

Strain relaxation in epitaxial Ge crystals grown on patterned Si(001) substrates



Yadira Arroyo Rojas Dasilva^{a,*}, Marta D. Rossell^a, Fabio Isa^{a,b}, Rolf Erni^a, Giovanni Isella^c, Hans von Känel^{a,b}, Pierangelo Gröning^d

^aElectron Microscopy Center, EMPA, Swiss Federal Laboratories for Materials Science and Technology, Überlandstrasse 129, Dübendorf CH-8600, Switzerland

^bLaboratory for Solid State Physics, ETH Zürich, Otto-Stern-Weg 1, Zürich CH-8093, Switzerland

^cL-NESS and Department of Physics, Politecnico di Milano and INFN-CNR, Via Anzani 42, Como I-22100, Italy

^dDepartment of Advanced Materials and Surfaces, EMPA, Swiss Federal Laboratories for Materials Science and Technology, Überlandstrasse 129, CH-8600 Dübendorf, Switzerland

ARTICLE INFO

Article history:

Received 15 August 2016

Accepted 4 September 2016

Available online xxxx

Keywords:

Dislocations
Stacking Faults
Twins
HAADF-STEM
Ge

ABSTRACT

In this paper we report on the defects formed in Ge crystals grown on Si(001) pillars upon strain relaxation. The analysis is performed by high-angle annular dark-field scanning transmission electron microscopy. The strain relaxation happens by means of 60° and 90° misfit dislocations with Burgers vectors $\vec{b} = \frac{1}{2}\langle 110 \rangle$. Misfit dislocations may split forming partial dislocations with Burgers vectors $\vec{b} = \frac{1}{6}\langle 112 \rangle$, and are separated by a stacking fault. Besides, intrinsic stacking faults in different {111} planes interact and annihilate each other forming stair rod dislocations. Coherent and incoherent twin boundaries of the $\Sigma 3\{111\}$ and $\Sigma 3\{112\}$ types are also found in the Ge.

© 2016 Elsevier Ltd. All rights reserved.

When Ge layers epitaxially grown on Si substrates reach a critical thickness, the misfit strain is accommodated by misfit dislocations (MDs) at the interface with their half planes in the Si-substrate. The MDs are of 60° and 90° types with Burgers vectors $\vec{b} = \frac{1}{2}\langle 110 \rangle$ lying in {111} planes and line direction along [110]. The MDs are always accompanied by threading dislocations [1] (TDs) which cross the layers and end at the Ge surface. The TDs are of 60°-type lying in {111} planes. Besides the TDs, planar defects have also been observed in Ge layers such as stacking faults (SFs) and twin boundaries (TBs) especially for low growth temperatures [2–4]. They are for example created at the interface during the recrystallization of Ge [2] or during the coalescence of islands during the growth [3,4].

As the performance of semiconductor devices is largely affected by dislocations, much effort is devoted to develop new methods for strain relief and to reduce the MD and TD densities. The approach pursued here is to grow three-dimensional (3D) Ge crystals on Si substrates patterned at a micrometer scale (i.e. Si pillars). The crystals are grown by low-energy plasma enhanced chemical vapor deposition (LEPECVD) far from equilibrium at high rates of around

15 μm/h and substrate temperatures of about 500 °C [5,6]. At substrate dimensions in the micrometer range the misfit strain is not reduced much in comparison to planar substrates, and MDs are still formed at the interface. However, the 60° TDs are eliminated because they end at the sidewalls of the Ge crystals [7]. Thus, the 60° TD density is reduced or even eliminated, depending on the height of the Ge crystals. Instead, new TDs are formed in the Ge which are identified as edge and screw dislocations with Burgers vectors $\vec{b} = \frac{1}{2}\langle 110 \rangle$ and $\vec{b} = [001]$, respectively [6,8,9]. So far, planar defects have not been reported in Ge crystals grown on Si pillars.

Based on transmission electron microscopy (TEM) and high-angle annular dark-field scanning transmission electron microscopy (HAADF-STEM), the present work provides a detailed analysis of the defects formed to relax the misfit strain in Ge crystals grown on Si(001) pillars.

The Ge crystals were grown on Si(001)-pillars with dimensions $5 \times 5 \mu\text{m}^2$ and 8 μm in height [5]. TEM cross sectional samples were prepared by mechanical polishing, dimple grinding, and ion milling using a Fischione ion mill model 1050 with 3 and 2 kV Ar ions to achieve electron transparency. TEM observations were carried out using a JEOL 2200FS TEM/STEM microscope operated at 200 kV, and a double spherical aberration-corrected JEOL JEM-ARM200F microscope operated at 200 kV for the HAADF-STEM analysis. The latter microscope was set up in STEM mode with a

* Corresponding author.

E-mail address: Yadira.Arroyo@empa.ch (Y. Arroyo Rojas Dasilva).

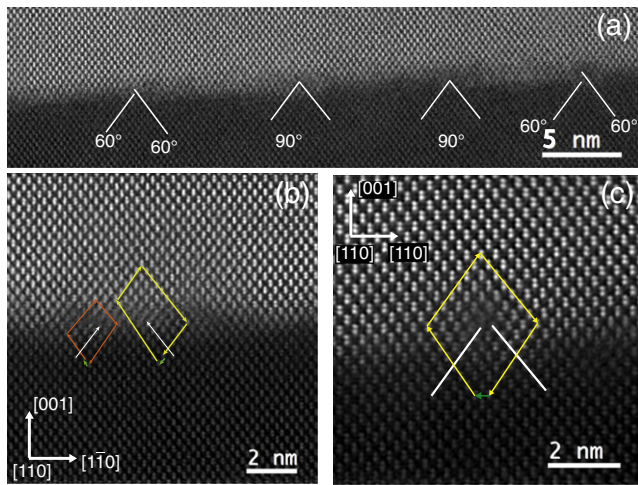


Fig. 1. HAADF-STEM images of the Ge/Si interface: a) Ge/Si interface showing the position of the 60° and 90° MDs with white lines, b) Burgers circuits of the 60° MDs (in red and yellow arrows) and Burgers vectors (green arrows) and c) Burgers circuit of the 90° MDs at the interface.

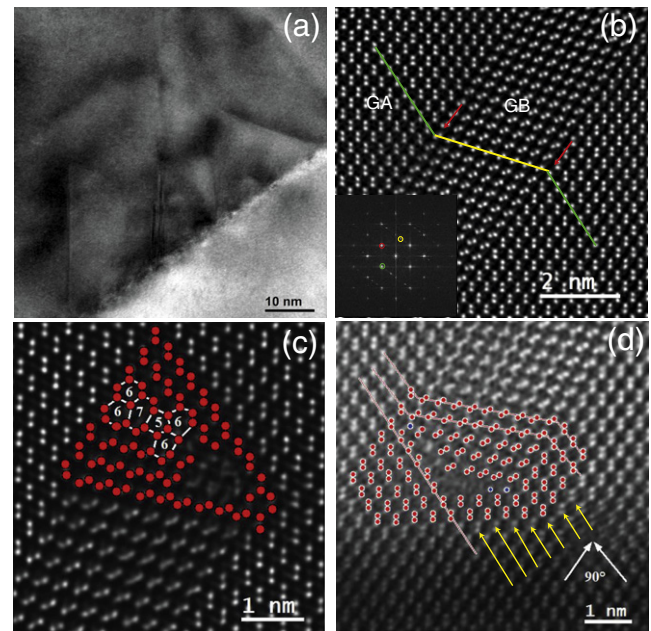


Fig. 2. High resolution images of a Ge crystal: a) HRTEM overview image of the Ge/Si interface with planar defects, b) HAADF-STEM image of two CTBs and its FFT, c) ITB closing the CTBs, and d) Ge/Si interface at the CTB. Dumbbells are denoted by red dots and partial misfit dislocations (PMDs) with yellow arrows. (For interpretation of the references to color in this figure legend, the reader is referred to the web version of this article.)

probe semi-convergence angle of 25.3 mrad and an annular semi-detection range of the annular dark-field detector of 90–370 mrad.

Fig. 1 (a) shows a HAADF-STEM image of the Ge/Si interface. It can be seen that the 4% lattice mismatch between the two materials is accommodated by the formation of MDs (white lines). The MDs are identified as pairs of perfect glissile 60° dislocations and perfect sessile 90° dislocations. The interface around the pairs is not smooth and steps of 2–3 atomic layers are observed. These steps are formed by the creation of the MDs at the interface that initially is flat [10]. In the pair of 60°, one of the 60° MD lies at the interface whereas the other is located in the Ge layer a few atomic layers above the interface; this is typical for films grown far from equilibrium [11]. The Burgers circuits of a pair of 60° MDs are shown in **Fig. 1** (b), using the (finish-start right-handed) FS/RH convention [12]. The Burgers vectors, indicated by green arrows, are $\vec{b} = \frac{1}{2}[\bar{1}01]$ and $\vec{b} = \frac{1}{2}[011]$. **Fig. 1** (c) shows the Burgers circuit and vector of a 90° MD; it is a Lomer dislocation lying in the (001) planes with $\vec{b} = \frac{1}{2}[\bar{1}10]$. The 90° MDs are formed by the interaction of two 60° MDs with Burgers vectors in different glide planes $\frac{1}{2}[\bar{1}01] + \frac{1}{2}[011] \rightarrow \frac{1}{2}[\bar{1}10]$. This reaction results in a reduction of the core and elastic energies ($a^2 > \frac{a^2}{2}$, where a is the lattice parameter). The 60° MDs are therefore strongly attracted to each other forming the 90° Lomer MD.

Besides MDs, a high density of planar defects was observed in the Ge crystals. **Fig. 2** (a) shows a HRTEM image of the Ge/Si interface with planar defects with a density of up to $1 \times 10^6 \text{ cm}^{-1}$. They are located on $(1\bar{1}1)$ and $(1\bar{1}\bar{1})$ planes and some of them look like pyramids with angles of 70.5° between them. These defects propagate along the $\{111\}$ planes with extensions between 3 to 40 nm. HAADF-STEM observations show that they are coherent twin boundaries (CTBs) of the $\Sigma 3\{111\}$ -type, as well as extrinsic and intrinsic stacking faults (ESFs and ISFs). The formation of these types of defects can be explained by island growth, impurities on the Si surface [13] or by splitting of 60° dislocations [11]. **Fig. 2** (b) shows CTBs in a Ge crystal formed at the interface with an extension of 40 nm. The TBs are pointed by red arrows and the $\{111\}$ plane orientations are shown by the green and yellow lines, passing from grain A (GA) to grain B (GB) and then again to GA. The area between the two CTBs corresponds to 9 atomic layers of $\{111\}$ planes (2.94 nm, assuming $a = 0.5676 \text{ nm}$). The inset of **Fig. 2** (b) shows the Fourier transform of the image. Here, the TB plane is $(1\bar{1}\bar{1})$ GA = $(1\bar{1}1)$ GB (red circle), and the planes corresponding to the GA and GB are $(1\bar{1}1)$ and $(1\bar{1}\bar{1})$, respectively (green

and yellow circles). The CTB ends inside the crystal (**Fig. 2** (c)), forming an incoherent twin boundary (ITB) of the $\Sigma 3\{112\}$ -type which is perpendicular to the $\Sigma 3\{111\}$ -CTB. The planes forming the ITB are $(1\bar{1}1)$ and $(1\bar{1}\bar{1})$ forming 7, 5 and 6 rings along the boundary. It is not possible to observe the whole length of the ITB in this figure due to the overlap of grains A and B. **Fig. 2** (d) shows an image of the CTB at the Ge/Si interface. Because this area is highly stressed, a clear observation of the atomic positions is not possible. Nevertheless, where visible, dumbbells are marked by red circles, single atomic columns with blue circles corresponding to partial dislocations (PDs) marked by yellow arrows, and continuous $(1\bar{1}1)$ planes are denoted by red lines. A twin is formed by the gliding of a group of Shockley PDs along parallel $\{111\}$ planes. The group of Shockley PDs are 30° type since the Ge grows initially compressed [14]. The Ge and Si planes at the interface in the twin seem to form a TB along the Ge/Si interface. According to our observations the CTBs are created at the Si surface due to the small steps around the pairs of MDs or during the coalescence of islands during the growth of the buffer layer at low temperature. This shows that for growth by LEPECVD at 500 °C, preferentially islands nucleate rather than a two-dimensional layer.

Fig. 3 (a) shows a HAADF-STEM image of the Ge/Si interface with a SF wherein the half planes of the 60° MDs in the substrate are marked with white arrows. A PMD is marked by red line limiting a SF. The stacking sequence of the SF (**Fig. 3** (b)) changes from AaBbCcAaBbCc... to AaBbCcBbAaBbCc..., where the bold Bb is an extra plane. Therefore, SF is of extrinsic type because there is an extra plane. Since Ge is compressively strained on the (001)-Si pillars, the dissociation of a 60° MD at the interface into two PMDs and an ESF leads to a 90° PMD at the interface and a 30° PMD in the Ge crystal in the vicinity of an additional perfect 60° MD [11,15,16]. The 60° MD is attracting the 90° PMD at the interface and repulsing the 30° PMD to the film [11]. **Fig. 3** (a) shows the position of the Shockley 90° PMD (red lines) at the interface, and nearby there is a 60° MD. A 90° MD with an ESF is equivalent to a pair of 30° MDs with an ISF

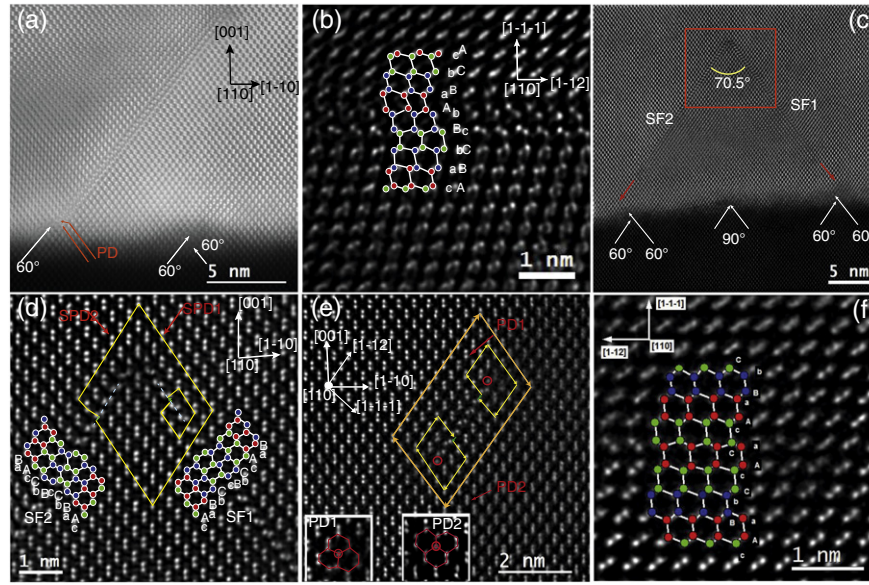


Fig. 3. HAADF-STEM images of the Ge crystal: a) PMD and ESF created at the Ge/Si interface, b) stacking sequence of the ESF, c) SFs interaction, d) image of the vertex of the SFs, e) a SF bounded by two SPDs, and f) magnified image showing the stacking sequence of the ISF. PD cores are magnified in the insets in Fig. 3(e), the colored dots are the atomic positions, the Burgers circuits and vectors are indicated by yellow and green arrows respectively.

on the adjacent glide planes [16]. The reaction of the splitting of the MD is $\frac{1}{2}[101] \rightarrow \frac{1}{6}[\bar{1}\bar{1}2] + \frac{1}{6}[211]$ which is favorable since there is a reduction of energy ($\frac{a^2}{2} > \frac{a^2}{3}$), where the first and second terms are the 90° and 30° PMDs, respectively.

We also observed interactions between SFs near the Ge/Si interface. When two SFs extend along the {111} planes with an acute angle of 70.5° in between, they annihilate each other in vertices forming stair rod dislocations (SRDs) (Fig. 4 (c)) [12]. The SF1 and SF2 are created by the coalescence of islands around MD pairs or, by the dissociation of a 60° or screw dislocations. The SFs are identified as intrinsic type (Fig. 3 (d)). The stacking sequence changes from

AaBbCcAaBbCc... to AaBbCcBbCcAaBbCc... where an Aa plane is missing in both SFs. For the SRD identification, the Burgers vector is obtained by the method described by Cottrell [17] for a dislocation at the boundary of two faults. It consists of two Burgers circuits, one constructed around the SF1 starting and finishing at the SF1, and the other one around the SF1 and SRD starting and finishing at the SF2 (dashed blue line). The Burgers vector of the SRD is the difference between them. The Burgers circuits and vectors of both faults are depicted by yellow lines and by green arrows. The step of the Burgers circuit in the faulted area is like the one in the good material. The Burgers vectors are found to be in {111} planes, the magnitude of the Burgers vectors is $\frac{1}{3}$ the distance of the projected lattice points along the $\langle 112 \rangle$ direction which correspond to 30° PDs [18]. They are Shockley PDs (SPDs) type with $\vec{b} = \frac{1}{6}[211]$ and $\vec{b} = \frac{1}{6}[\bar{1}\bar{2}\bar{1}]$, therefore the Burgers vector of the SRD is given by $\frac{1}{6}[211] + \frac{1}{6}[\bar{1}\bar{2}\bar{1}] \rightarrow \frac{1}{6}[\bar{1}\bar{1}0]$ which implies an energy reduction $\frac{a^2}{3} > \frac{a^2}{18}$.

The configuration of the Shockley PDs with an intrinsic SF present in compressively strained materials is 30° PD at the interface and 90° PD in the compressed film having small separations [16,19]. Since the PDs forming the SRD are two 30°, they are not formed by the splitting of a 60° MD. In order to have 30° PDs in the Ge, a screw MD splits into two 30° MPDs [18,20]. Possible reactions of the splitting of the screw MDs [18] in the {111} planes are $\frac{1}{2}[110] \rightarrow \frac{1}{6}[211] + \frac{1}{6}[12\bar{1}]$ and $\frac{1}{2}[110] \rightarrow \frac{1}{6}[2\bar{1}1] + \frac{1}{6}[121]$, ($\frac{a^2}{2} > \frac{a^2}{3}$).

SFs inside the Ge crystals are also found but they are rarer than at the interface. They are located above the interface (≈ 20 nm) and bounded by two PDs. Fig. 3 (e) shows a HAADF-STEM image of a SF bounded by two PDs pointed by red arrows and separated by 2.63 nm. The general Burgers circuit (orange arrows) around the two PDs is a closed loop. This implies that Burgers vector is equal to zero along this projection indicating a null edge component. The Burgers circuit for each PD is depicted by yellow arrows. The projection of the Burgers vectors closing the circuits is $\vec{b} = \frac{1}{6}(112)$ (green arrows) which correspond to SPDs. The core structures of the SPDs are shown in the insets of Fig. 3 (e) where the half plane ends in a single atomic column (red circle). The two cores are similar and correspond to 30° type [21]. The magnitude of the Burgers vector

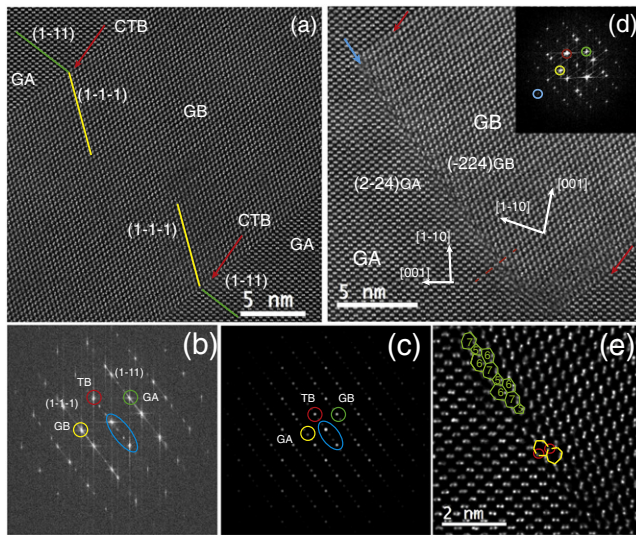


Fig. 4. Images of the Ge deposited on the sidewalls of the Si pillars: a) HAADF-STEM image of two CTBs, b) Fourier transform of the image in panel (a), c) simulation of the diffraction pattern of GA and GB in an epitaxial material, d) HAADF-STEM image of an ITB $\Sigma 3(112)$ and its FFT, e) magnified image from the ITB of panel (d) showing 5, 7 and 6 rings at the boundary. Red circles show the position in the rings of the single atomic columns.

of both PDs is $\frac{1}{3}$ the distance of the projected lattice points along the $\langle 112 \rangle$ direction which correspond to 30° PDs [18]. Since the general Burgers vector is zero, the splitting dislocation into SPDs is a screw dislocation. The Burgers vectors of the 30° SPDs correspond to $\vec{b} = \frac{1}{6}[211]$ and $\vec{b} = \frac{1}{6}[12\bar{1}]$. The splitting reaction is given by $\frac{1}{2}[110] \rightarrow \frac{1}{6}[211] + \frac{1}{6}[12\bar{1}]$ [18,22] implying again a reduction of energy $\frac{a^2}{2} > \frac{a^2}{3}$.

A magnified image of the stacking sequence is shown in Fig. 3 (f). The sequence of the atomic positions is shown by colored circles, where the normal stacking sequence AaBbCcAaBbCc... changes to AaBbCcAaCcAaBbCc... (Bb plane is missing), therefore, this fault is an ISF.

During the growth of the Ge crystals, Ge is also deposited on the sidewalls of the Si pillars producing an overgrowth area between the Ge in the sidewalls and the Ge crystal. CTBs are also found in this area with longer extension than those found at the interface (Fig. 4). They are located at the edge of the Si pillars and glide along $\{111\}$ planes across the overgrowth area. They end at the sidewalls or inside of the Ge crystals with an ITB of the $\Sigma 3\{112\}$ -type similar to Fig. 2 (c) [23–25]. In Fig. 4 (a), the CTBs, marked by red arrows, correspond to $(\bar{1}\bar{1}\bar{1})\text{GA} = (\bar{1}\bar{1}\bar{1})\text{GB}$ planes. The plane orientation in the GA $(\bar{1}\bar{1}\bar{1})$ and in the GB $(\bar{1}\bar{1}\bar{1})$ is marked by green and yellow lines, respectively. The area between the two CTBs contains 48 $\{111\}$ -planes (15.68 nm). Fig. 4 (b) shows the Fourier transform of the image in Fig. 4 (a), the TB planes correspond to $(\bar{1}\bar{1}\bar{1})\text{GA} = (\bar{1}\bar{1}\bar{1})\text{GB}$ (red circle), and the planes in GA and GB are $(\bar{1}\bar{1}\bar{1})$ and $(\bar{1}\bar{1}\bar{1})$, respectively (green and yellow circles). This image shows a periodicity of extra spots between the reflections (blue area). These extra spots are due to dynamical diffraction caused by the overlapping of the GA and GB grains. A simulated diffraction pattern calculated by JEMS [26] is shown in Fig. 4 (c) for an epitaxial material (GA + GB) including double diffraction effects. This simulated diffraction pattern shows a good match with the image in Fig. 4 (b). The CTBs end inside the crystal by closing with an ITB (Fig. 4 (d)). The CTBs are marked by red arrows and the ITB by a blue arrow. The ITB plane corresponds to $(\bar{2}\bar{2}\bar{4})\text{GA} = (\bar{2}\bar{2}\bar{4})\text{GB}$ shown in the Fourier transform (FFT) with a blue circle, the red circle corresponds to the $(\bar{1}\bar{1}\bar{1})\text{GA}$ and $(\bar{1}\bar{1}\bar{1})\text{GB}$ planes crossing the ITB. The green and yellow circles are $(\bar{1}\bar{1}\bar{1})$ in GA and $(\bar{1}\bar{1}\bar{1})$ in GB forming the ITB. Fig. 4 (e) shows the ITB structure which is periodic and formed by one 5 ring, one 7 ring and one distorted 6 ring [23]. The single atomic columns are pointed by red circles and are located at the corners of the 6 and 7 rings (yellow rings) in agreement with the model proposed by Sawada for Si [23].

In conclusion, defects at the Ge/Si interface were identified using HAADF-STEM analysis. The misfit strain in Ge crystals grown on (001) -Si patterned substrates is accommodated by MDs of 60° and 90° types lying on $\{111\}$ and $\{001\}$ planes. MDs split into SPDs bounding intrinsic or extrinsic SFs. The SFs annihilate when they meet each other on different $\{111\}$ planes forming a SRD. $\{111\}$ -CTBs are also found in the Ge crystals. They are created at the interface and end inside of the crystal with a $\{112\}$ -ITB.

Overall it can be concluded that the variety of 1D and 2D crystal defects in Ge crystals epitaxially grown far from equilibrium is greater than previously documented. The presence of these defects and the variety makes it difficult to estimate their impact on the physical properties of the Ge crystals.

Acknowledgments

Financial support by the Sinergia project NOVIPIX of the Swiss National Science Foundation (CRSII2 147639) and ETH Research Grant No. ETH-2011-2 is acknowledged. Access to the TEM facilities at IBM Research-Zurich, Switzerland, under the IBM/Empa Master Joint Development Agreement is gratefully acknowledged.

References

- [1] Y. Bolkhovityanov, A. Deryabin, A. Gutakovskii, L. Sokolov, *J. Cryst. Growth* 310 (2008) 3422–3427.
- [2] R. Duffy, M. Shayesteh, B. McCarthy, A. Blake, M. White, J. Scully, R. Yu, A.-M. Kelleher, M. Schmidt, N. Petkov, L. Pelaz, L.A. Marques, *Appl. Phys. Lett.* 99 (2011) 131910.
- [3] D. Leonhardt, S. Ghosh, S.M. Han, *J. Appl. Phys.* 110 (2011) 073516.
- [4] Y. Nakamura, A. Murayama, M. Ichikawa, *Cryst. Growth Des.* 11 (2011) 3301–3305.
- [5] C.V. Falub, H. von Känel, F. Isa, R. Bergamaschini, D. Chrastina, A. Marzegalli, G. Isella, E. Müller, P. Niedermann, L. Miglio, *Science* 335 (2012) 1330–1334.
- [6] A. Marzegalli, F. Isa, H. Groiss, E. Müller, C.V. Falub, A.G. Taboada, P. Niedermann, G. Isella, F. Schaeffler, F. Montalenti, H. von Känel, L. Miglio, *Adv. Mater.* 25 (2013) 4408–4412.
- [7] F. Isa, A. Marzegalli, A. Taboada, C. Falub, G. Isella, F. Montalenti, L. Miglio, *APL Mater.* 1 (2013) 052109.
- [8] H. Groiss, M. Glaser, A. Marzegalli, F. Isa, G. Isella, L. Miglio, F. Schaeffler, *Microsc. Microanal.* 3 (2015) 637–645.
- [9] Y. Arroyo-Rojas-Dasilva, M.D. Rossell, D. Keller, P. Gröning, F. Isa, T. Kreiliger, H. von Känel, G. Isella, R. Erni, *Appl. Phys. Lett.* 107 (2015) 093501.
- [10] M. Ichimura, J. Narayan, *Mater. Sci. Eng. B* 31 (1995) 299–303.
- [11] S. Oktyabrsky, J. Narayan, *Philos. Mag. A* 72 (1995) 305–314.
- [12] J.P. Hirth, J. Lothe, *Theory of the Dislocations*, 2nd ed., Wiley and Sons, USA, 1982.
- [13] P. Pirouz, F. Ernst, T. Cheng, *Mater. Res. Soc. Symp. Proc.* 116 (1988) 57.
- [14] L. Liu, Y. Zhang, T.-Y. Zhang, *J. Appl. Phys.* 101 (2007) 063501.
- [15] S. Oktyabrsky, J. Narayan, *Mater. Res. Soc. Symp. Proc.* 399 (1996) 443–448.
- [16] M. Ichimura, J. Narayan, *Philos. Mag. A* 73 (1996) 767–778.
- [17] A.H. Cottrell, *Theory of Crystal Dislocations*, 1st ed., Gordon and Breach, 1964.
- [18] X.-Y. Wan, J.-W. Liang, M.-L. Liu, X.-J. Jin, *Phys. Rev. B* 55 (1997) 9259–9262.
- [19] X. Zhang, Z. Zhang, *Progress in Transmission Electron Microscopy 2*, Surface Science, 1st ed., Springer, 2001.
- [20] P. Han, J. Zou, *Appl. Phys. Lett.* 72 (1998) 2424–2426.
- [21] P. Lu, D.J. Smith, *Philos. Mag. B* 64 (1990) 435–450.
- [22] J. Hornstra, *J. Phys. Chem. Solids* 5 (1958) 129–141.
- [23] H. Sawada, H. Ichinose, M. Kohyama, *J. Electron Microsc.* 51 (2002) 353–357.
- [24] A. Bourret, *J. Phys.* 46 (1985) C4–27–C4–38.
- [25] A. Bourret, J.J. Backman, *Trans. Jpn. Inst. Metals* 27 (1986) 125–134.
- [26] P. Stadelmann, *Microsc. Microanal.* 9 (2003) 60–61.